

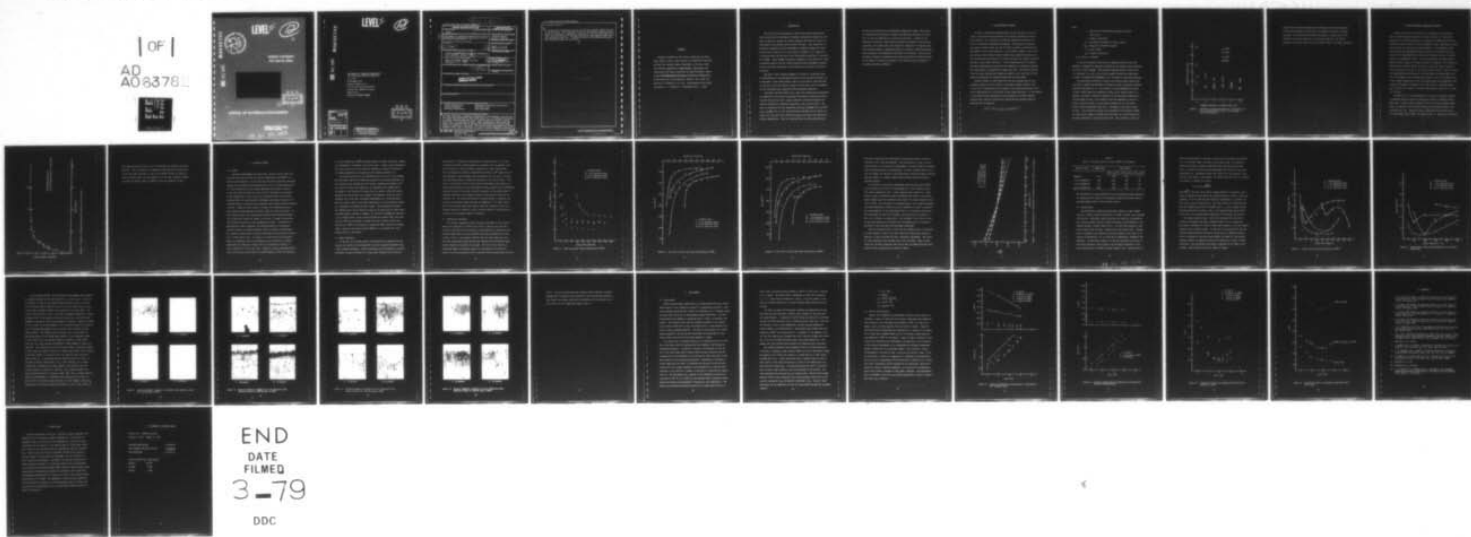
AD-A063 782

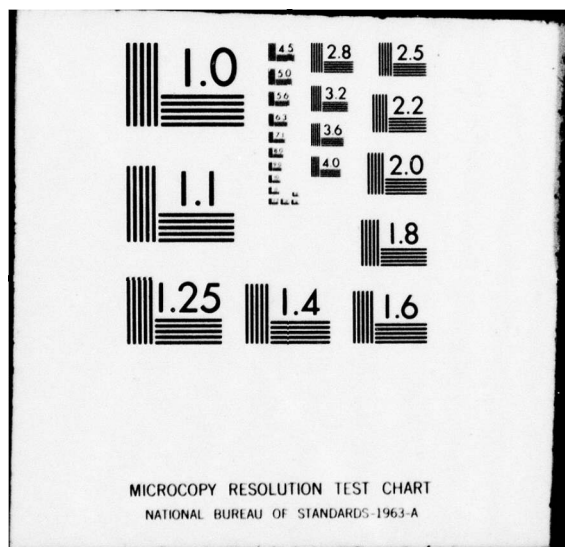
PURDUE UNIV LAFAYETTE IN TURNER LAB FOR ELECTROCERAMICS F/6 9/1  
THE EFFECTS OF SUBSTRATE COMPOSITION ON THICK FILM CIRCUIT RELI--ETC(U)  
NOV 78 R W VEST N00019-78-C-0236

NL

UNCLASSIFIED

| OF |  
AD  
AO 63782





AD A063 782

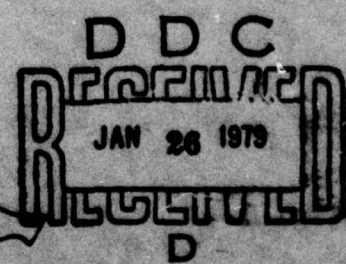
DOC FILE COPY.



LEVEL IV

12  
4

PURDUE UNIVERSITY  
West Lafayette, Indiana



SCHOOL OF MATERIALS ENGINEERING

APPROVED FOR PUBLIC RELEASE  
Distribution Unlimited

79 01 22, 068

**DDC FILE COPY**

**AD A0 63782**

**LEVEL II**

**(P)**

**THE EFFECTS OF SUBSTRATE COMPOSITION  
ON THICK FILM CIRCUIT RELIABILITY**

**R. W. Vest**

**30 November 1978**

**Quarterly Report No. 3**

**For the period 8/1/78-10/31/78**

**Contract No. N00019-78-C-0236**

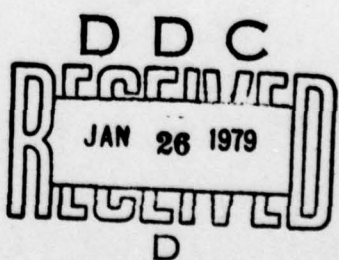
**Prepared for**

**NAVAL AIR SYSTEMS COMMAND**

REF ID: A6250000	
TYPE	DATA SHEET
EDITION	REV B
MANUFACTURED	00
NOTIFICATION	
BY	
DISTRIBUTION/AVAILABILITY CODE	
GENL	AVAIL AND OR SPECIAL
A	

**DISTRIBUTION STATEMENT A**

**Approved for public release;  
Distribution Unlimited**



Quarterly rept. no. 3,  
1 Aug-31 Oct 78,

**SECURITY CLASSIFICATION OF THIS PAGE (When Data Entered)**

REPORT DOCUMENTATION PAGE		READ INSTRUCTIONS BEFORE COMPLETING FORM
1. REPORT NUMBER Three ✓	2. GOVT ACCESSION NO.	3. RECIPIENT'S CATALOG NUMBER
4. TITLE (and Subtitle) <b>THE EFFECTS OF SUBSTRATE COMPOSITION ON THICK FILM CIRCUIT RELIABILITY</b>		5. TYPE OF REPORT & PERIOD COVERED Quarterly Report 8/1/78 - 10/31/78
7. AUTHOR(s) R. W. Vest	6. PERFORMING ORG. REPORT NUMBER N00019-78-C-0236	
8. CONTRACT OR GRANT NUMBER(s)	15	
9. PERFORMING ORGANIZATION NAME AND ADDRESS <del>PURDUE RESEARCH FOUNDATION, PURDUE UNIVERSITY</del> West Lafayette, Indiana 47907	10. PROGRAM ELEMENT, PROJECT, TASK AREA & WORK UNIT NUMBERS Turner Lab	
11. CONTROLLING OFFICE NAME AND ADDRESS NAVAL AIR SYSTEMS COMMAND, AIR 310B Washington, D. C. 20361	12. REPORT DATE 30 Nov 1978	
14. MONITORING AGENCY NAME & ADDRESS (if different from Controlling Office)	13. NUMBER OF PAGES 37	
16. DISTRIBUTION STATEMENT (of this Report)  <b>APPROVED FOR PUBLIC RELEASE: DISTRIBUTION UNLIMITED</b>	15. SECURITY CLASS. (of this report)	
17. DISTRIBUTION STATEMENT (of the abstract entered in Block 20, if different from Report)	15a. DECLASSIFICATION/DOWNGRADING SCHEDULE	
18. SUPPLEMENTARY NOTES		
19. KEY WORDS (Continue on reverse side if necessary and identify by block number)		
Thick Film Resistors Ceramic Substrates Electrical Resistivity	Temperature Coefficient Resistivity Electronic Glass Glass Sintering	
20. ABSTRACT (Continue on reverse side if necessary and identify by block number)		
The sheet resistance, temperature dependence of the resistance, and the current noise were measured for thick film resistors as a function of the amount of alumina substrate dissolved in the resistor glass for resistor firing times from 4 to 22 minutes at 800°C. Large variations in these three properties were observed, and the changes were qualitatively correlated with changes in viscosity of the glass. The microstructure development and charge transport model used to correlate the results involves changing proportions		

**DD FORM 1 JAN 73 1473 EDITION OF 1 NOV 68 IS OBSOLETE**  
**S/N 0102-014-6691 |**

**SECURITY CLASSIFICATION OF THIS PAGE (When Data Entered)**

20 Abstract (cont'd)

of sintered and non-sintered contacts in the RuO<sub>2</sub> networks within the body of the resistors. The solubility of RuO<sub>2</sub> in the resistor glass was determined as a function of temperature and amount of substrate dissolved in the glass, and the kinetics of substrate dissolution were measured under varying processing conditions. Preliminary results on MIM devices fabricated with resistor glasses are presented.



#### FOREWORD

Research described in this report constitutes the third three months of effort under Contract No. N00019-78-C-0236 with the Naval Air Systems Command, Department of the Navy, under the technical cognizance of James Willis. The research was conducted in the Turner Laboratory for Electroceramics, School of Materials Engineering and School of Electrical Engineering, Purdue University, West Lafayette, Indiana 47907, under the direction of Professor R. W. Vest. Contributing to the project were Messrs. J. M. Himelick, P. Palanisamy and R. L. Reed.

## 1. INTRODUCTION

The print and fire processing of thick film circuits ensures that there always will be some degree of chemical interaction between the film and the substrate, because all common substrate materials are soluble to some degree in the glasses used in thick film inks. This interaction is primarily responsible for the development of adhesion between the thick film and the substrate, but it also leads to changes in the composition of the glass with the net result that the physical properties of the glass will change. These changes in physical properties of the glass will result in modified kinetics for the various microstructure development processes and all electrical properties of the resistors are related to the micro-structure.

The goal of this research program is to develop a sufficient level of understanding of the phenomena involved so that appropriate models can be developed. These models should lead to the writing of specifications for impurity limits and additive ranges for substrates, and to recommendations concerning glass composition and processing conditions.

Previously reported studies (1-4) under this program have established the magnitude of the effects resulting from chemical interaction between a thick film resistor and a ceramic substrate, and have determined the specific influence on important properties of the resistor glass. The rates of dissolution of two substrates, 96%  $\text{Al}_2\text{O}_3$  (AlSiMag 614) and 99.5%  $\text{Al}_2\text{O}_3$  (AlSiMag 772), in two lead borosilicate glasses (63 w/o  $\text{PbO}$ -25 w/o  $\text{B}_2\text{O}_3$ -12 w/o  $\text{SiO}_2$  and 70 w/o  $\text{PbO}$ -20 w/o  $\text{B}_2\text{O}_3$ -10 w/o  $\text{SiO}_2$ ) were measured at various temperatures. The rate limiting steps for each substrate-glass

system were determined in all appropriate temperature ranges, and analytical equations were developed to predict the substrate recession as a function of time and temperature for thick film resistors. Studies of the influence of substrate constituents dissolved in the glass on the physical properties of the glass and on the electrical properties of resistors made from the glass showed a significant effect on viscosity, sintering kinetics, sheet resistance and temperature coefficient of resistance. The viscosity and sheet resistance increased and the sintering kinetics and TCR decreased as the amount of substrate dissolved in the resistor glass increased for the same processing conditions.

## 2. RuO<sub>2</sub> SOLUBILITY STUDIES

In order to develop an adequate model for the influence of the substrate on microstructure development and electrical properties of thick film resistors, it is necessary to know the influence of dissolved substrate on conductive ripening and sintering. Sintering and ripening of the conductive phase (RuO<sub>2</sub>) are the two final processes in microstructure development of thick film resistors. In the initial stages of the sintering process, necks develop between adjacent RuO<sub>2</sub> conductive particles; as the sintering process proceeds, the necks grow until the adjacent particles coalesce to form larger particles. In the ripening process, the smaller particles preferentially dissolve and the material is transported through the liquid phase to precipitate on larger particles. The primary driving force for both sintering and ripening processes is the reduction in interfacial area between the conductive phase and the glass phase.

Earlier studies (5) have shown that the rate limiting step for the ripening of RuO<sub>2</sub> in 63-25-12 glass is the phase boundary reaction, that is, the rate of dissolution at the surface of the smaller particles or the rate of precipitation at the surface of the larger particles. If the kinetics of the initial stage sintering are also governed by the phase boundary reaction rate, then the relative neck growth between adjacent spherical particles will be given by

$$(x/r)^4 = (8 k_1 C_o \gamma_{sl} V_o K_T / k_2 RT) r^{-2} t$$

where

$x$  = radius of the neck between adjacent particles

after time  $t$

$r$  = radius of particles

$C_o$  = equilibrium solubility of  $\text{RuO}_2$  in glass

$\gamma_{s1}^A$  =  $\text{RuO}_2$ -glass interfacial energy

$V_o$  = molar volume

$K_T$  = transfer coefficient

$R$ ,  $k_1$  and  $k_2$  = constants

It was also observed in the earlier ripening studies (6) that the presence of AlSiMag 614 substrate dissolved in the resistor glass decreased the rate of  $\text{RuO}_2$  ripening. The decreased ripening kinetics could be due to a decrease in  $C_o$ ,  $\gamma_{s1}^A$  or  $K_T$ , and the present studies were undertaken in order to determine the dependence of  $C_o$  on amount of dissolved substrate.

The equilibrium solubility of  $\text{RuO}_2$  in the various glass compositions from  $700^\circ$  to  $1000^\circ\text{C}$  was determined utilizing an atomic absorption technique previously described (3, 7). The results of these experiments are given in Fig. 1 which shows the solubility of  $\text{RuO}_2$  in the resistor glass as a function of amount of dissolved substrate at four different temperatures. The data shown in Fig. 1 are consistent with the magnitude of the solubility reported for  $\text{RuO}_2$  in soda-silicate glasses (8, 9), and in the 63-25-12 lead borosilicate glass (10). According to the results shown in Fig. 1, the solubility of  $\text{RuO}_2$  in the standard 63-23-12 glass at  $800^\circ\text{C}$  is 9 ppm, which compares favorably with the result of 10 ppm obtained for the same conditions in the earlier work (10). The solubility is seen to

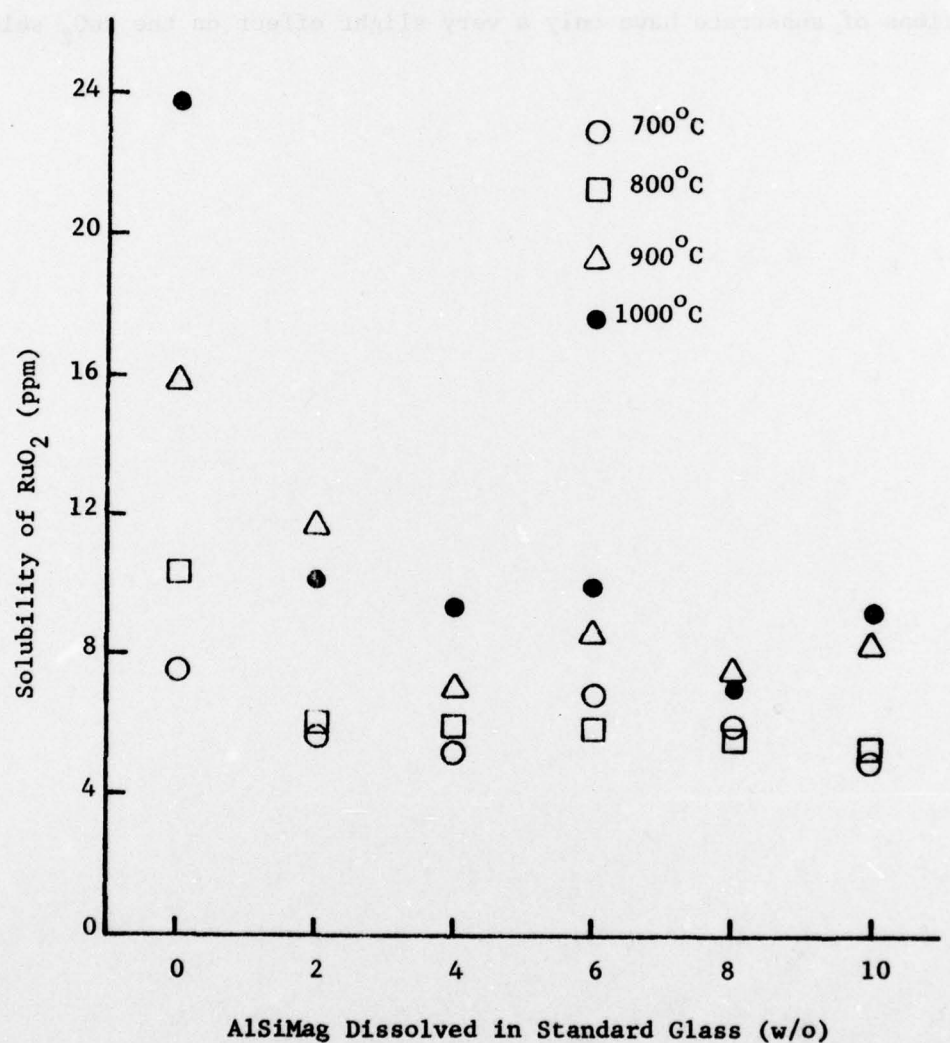


**Figure 1.** Influence of Dissolved Substrate on Solubility of RuO<sub>2</sub> in Standard (63 w/o PbO - 25 w/o B<sub>2</sub>O<sub>3</sub> - 12 w/o SiO<sub>2</sub>) Glass.

increase with increasing temperature and decrease with increasing amount of dissolved substrate, but the effect of dissolved substrate is highly nonlinear. The solubility decreases very sharply to nearly half of the original value with an addition of two percent substrate, but further additions of substrate have only a very slight effect on the RuO<sub>2</sub> solubility.

### 3. RESISTOR SUBSTRATE INTERACTION KINETICS

Results for the rate of dissolution of substrates in bulk glasses and in resistor films were given in a previous report (2). Empirical expressions for substrate recession as a function of temperature and glass composition were developed for short interaction times, from which recession-time profiles for resistor films were predicted. The agreement between the predicted and experimental results was good for very short and long times, but the experimental data points fell slightly above the predicted profile for intermediate times. It was proposed that the higher experimental recession values for actual resistors as compared to the predictions based on data from bulk glasses were due to agitation, which is known to occur in resistor films due to the release of gas bubbles. Earlier studies (11) demonstrated the evolution of the gas bubbles from glass-RuO<sub>2</sub> resistors, and suggested that the three most likely sources of the bubbles were: 1) air trapped during pore closure occurring during the intermediate stage of glass sintering; 2) oxidation of the last traces of screening agent; and 3) evolution of volatile ruthenium oxides (RuO<sub>2</sub> or RuO<sub>3</sub>) due to oxidation of RuO<sub>2</sub>.

Possibility No. 3 was investigated as a source of agitation leading to enhanced recession rates by repeating the resistor recession measurements with a resistor paste containing glass as the only inorganic ingredient, as opposed to the 95% glass-5% RuO<sub>2</sub> in the resistor paste of the previous study (2). These new results, along with the previous results for the 5% RuO<sub>2</sub> film at 840°C, are shown in Fig. 2. These results indicate

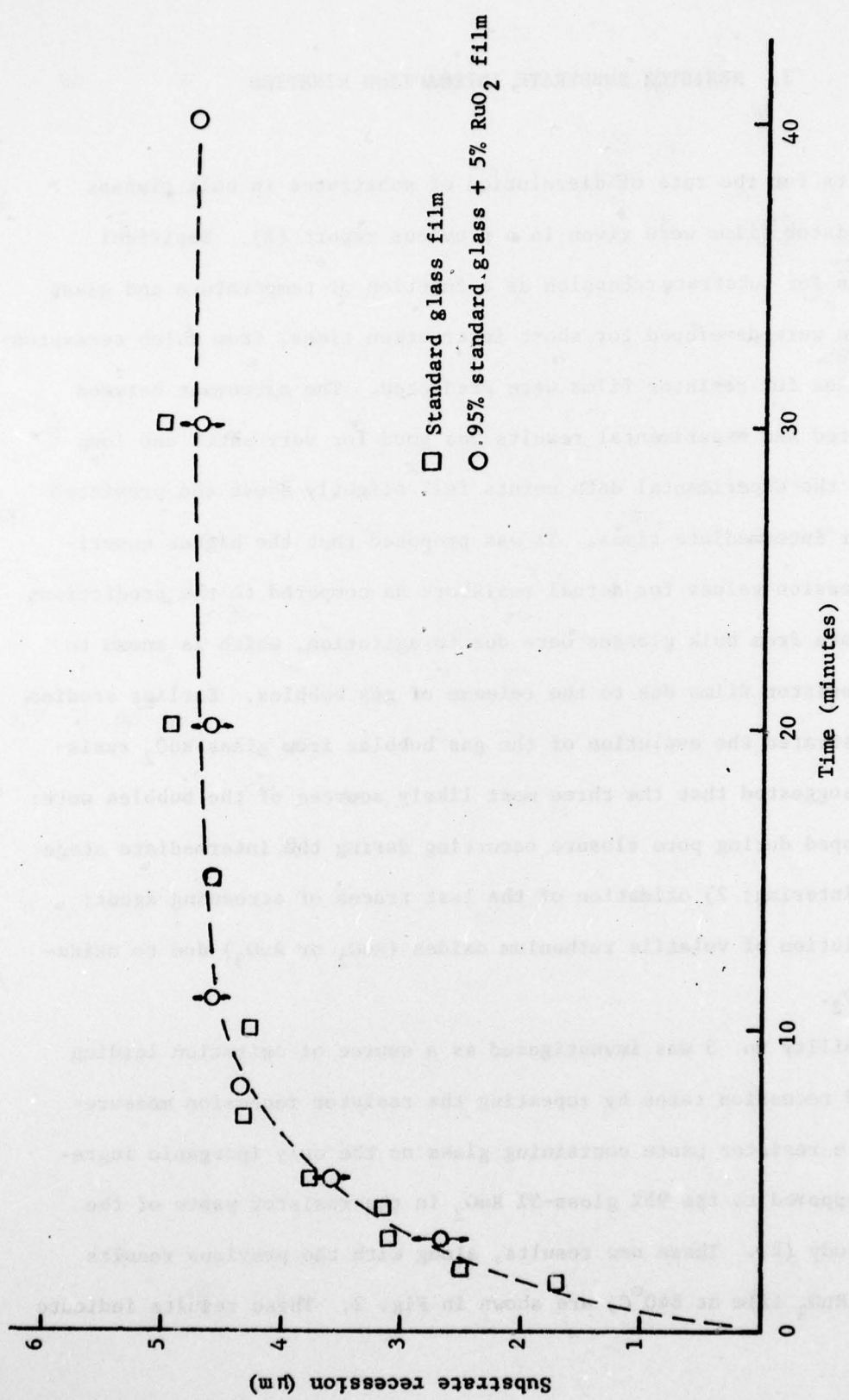


Figure 2. Kinetics of Substrate Recession in Resistor Films at  $840^{\circ}\text{C}$ .

that RuO<sub>2</sub> particles in the film do not influence the substrate recession kinetics. This conclusion is in agreement with qualitative observations on the hot stage microscope of the rate of bubble release for resistors with and without RuO<sub>2</sub>; the rate appears to be the same, therefore suggesting that the primary source of bubbles is not the oxidation of RuO<sub>2</sub>.

#### 4. RESISTOR STUDIES

##### 4.1 General

Electrical measurements were previously reported (4) for thick film resistors that had been fired at various temperatures ( $700^{\circ}$ - $900^{\circ}$ C) for a fixed time (10 minutes). It was found that the sheet resistance decreased rapidly with increasing firing temperature at the low firing temperatures, and then levelled off as the firing temperature was further increased. It was also found that both hot and cold TCR's increased for increasing firing temperatures. These results are consistant with the previously developed model for microstructure development and charge transport (12) involving chains of  $\text{RuO}_2$  particles containing both sintered and non-sintered contacts. During the early stages of firing, the conducting particles come together forming chains and quickly reduce the sheet resistance. As the firing proceeds, more non-sintered contacts become sintered contacts but no additional chains are formed, so the rate of change of resistance with further increases in firing temperature is small. In addition to decreasing the sheet resistance, the decreased number of non-sintered contacts relative to sintered contacts cause an increase in TCR because the sintered contacts have a positive TCR whereas the non-sintered contacts have a large negative TCR. According to the microstructure development model, an equivalent state of development can be achieved at a constant temperature by firing for a longer time as is obtained by firing at a higher temperature for the same time. During the present reporting period, thick film resistors were fired for varying lengths of time (3-22 minutes)

at a fixed temperature ( $800^{\circ}\text{C}$ ) and then tested for sheet resistance, temperature dependence of resistance and current noise. Current noise measurements were also carried out on the resistors prepared by firing for 10 minutes at varying temperatures as reported in the previous quarterly (4).

The substrates used for all experiments were  $0.5 \times 13 \times 13$  mm AlSiMag 614 with DuPont 9885 Pt-Au conductive prepared as previously described (4). The substrates were divided into four groups, numbered and weighed; after the resistor firings were completed, the substrates were weighed again. The weight of the resistor film along with its density, width and length, permitted the calculation of an average film thickness, which was used to normalize all of the sheet resistance measurements to a  $25 \mu\text{m}$  thickness. The four resistor inks, of the same compositions as in the previous studies (4), contained 5 w/o  $\text{RuO}_2$  relative to glass. One formulation contained the standard glass (63 w/o  $\text{PbO}$ -25 w/o  $\text{B}_2\text{O}_3$ -12 w/o  $\text{SiO}_2$ ) and the other three contained glasses produced by adding 4, 6, and 10 w/o AlSiMag 614 substrate to the standard glass. After screen printing the resistor inks, they were dried at  $130^{\circ}\text{C}$  for 30 minutes to remove the butyl carbitol solvent and then dried at  $300^{\circ}\text{C}$  for 30 minutes to remove the ethyl cellulose screening agent. Resistors were batch fired at  $800^{\circ}\text{C}$  in a box furnace for times varying from 3 to 22 minutes.

#### 4.2 Sheet Resistance

At the end of the firing period, the resistors were removed from the furnace, air cooled to room temperature, and the resistance measured using a four terminal technique. From the resistance and the geometry, the sheet resistance in ohms per square for a  $25 \mu\text{m}$  film thickness was calculated

and plotted as a function of firing time, as shown in Fig. 3. All four formulations showed a rapid decrease in resistance with increasing firing time followed by a fairly constant resistance for longer firing times. The time required to develop a measureable resistance ( $10^{11}$  ohms) and the time required to reach constant sheet resistance are both seen to increase with increasing amount of substrate dissolved in the resistor glass. This result is consistent with the microstructure development model which predicts reduced kinetics for the development of  $\text{RuO}_2$  networks with predominately sintered contacts as the glass viscosity increases; an increased amount of substrate dissolved in the standard glass has been shown to increase the viscosity (4). The observation that an increased amount of substrate dissolved in the resistor glass increases the magnitude of the sheet resistance in the constant region may indicate that the resistance of the non-sintered contacts in addition to their relative number in the  $\text{RuO}_2$  chains increases with increasing amount of substrate.

#### 4.3 Temperature Dependence

The constant temperature baths previously described (4) were used to measure the resistance at  $125^\circ\text{C}$  and at  $-55^\circ\text{C}$  so that hot and cold TCRs could be calculated for the resistors of differing glass compositions and varying firing times; the data obtained from these experiments are shown in Figs. 4 and 5. Both figures indicate that the TCR becomes more positive with increasing firing time and more negative with increasing weight percent substrate dissolved in the glass. The first result implies an increasing number of sintered contacts at the expense of non-sintered contacts as firing proceeds because a sintered contact between  $\text{RuO}_2$  particles

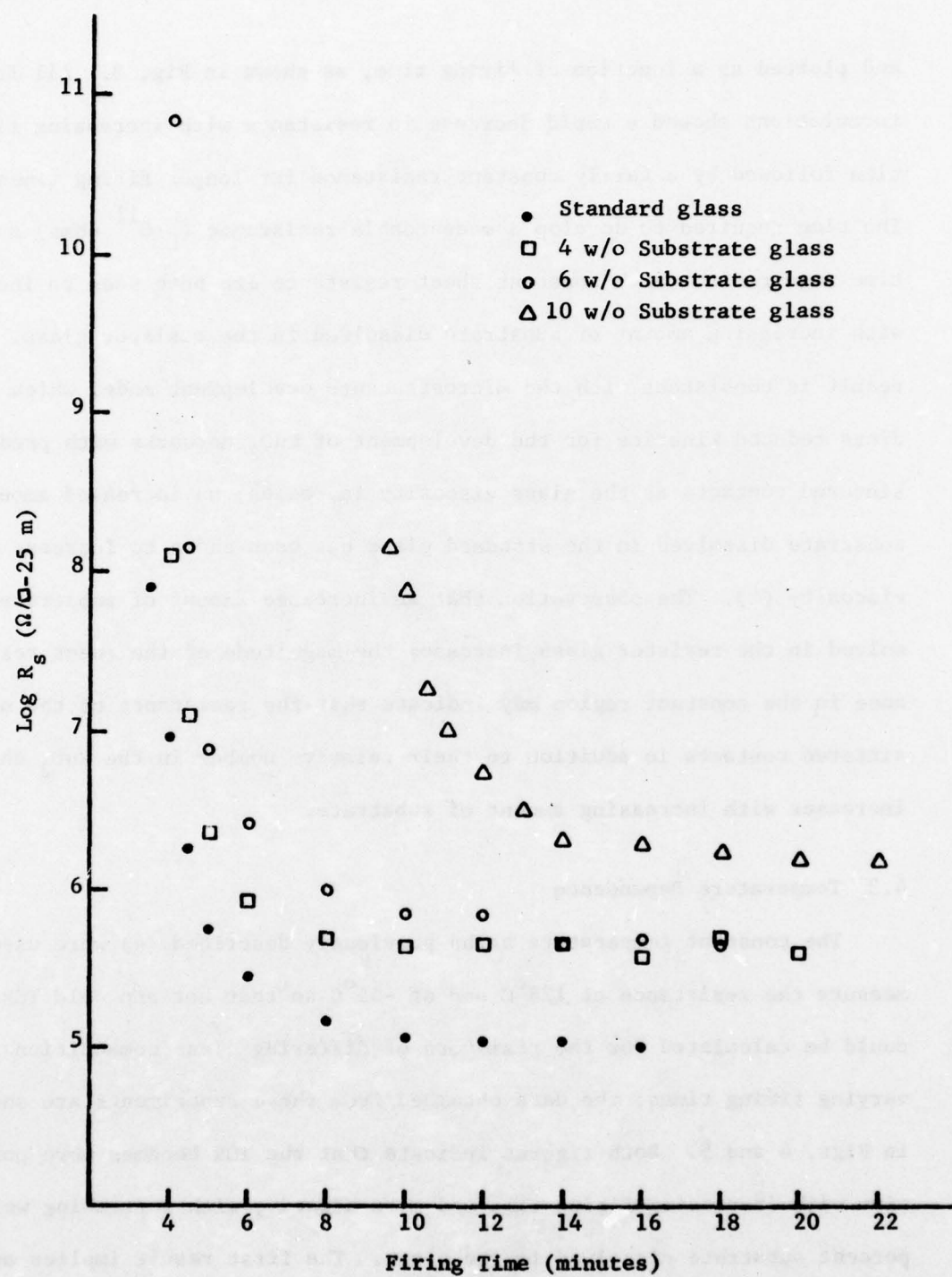


Figure 3. Sheet Resistance versus Firing Time at 800°C.

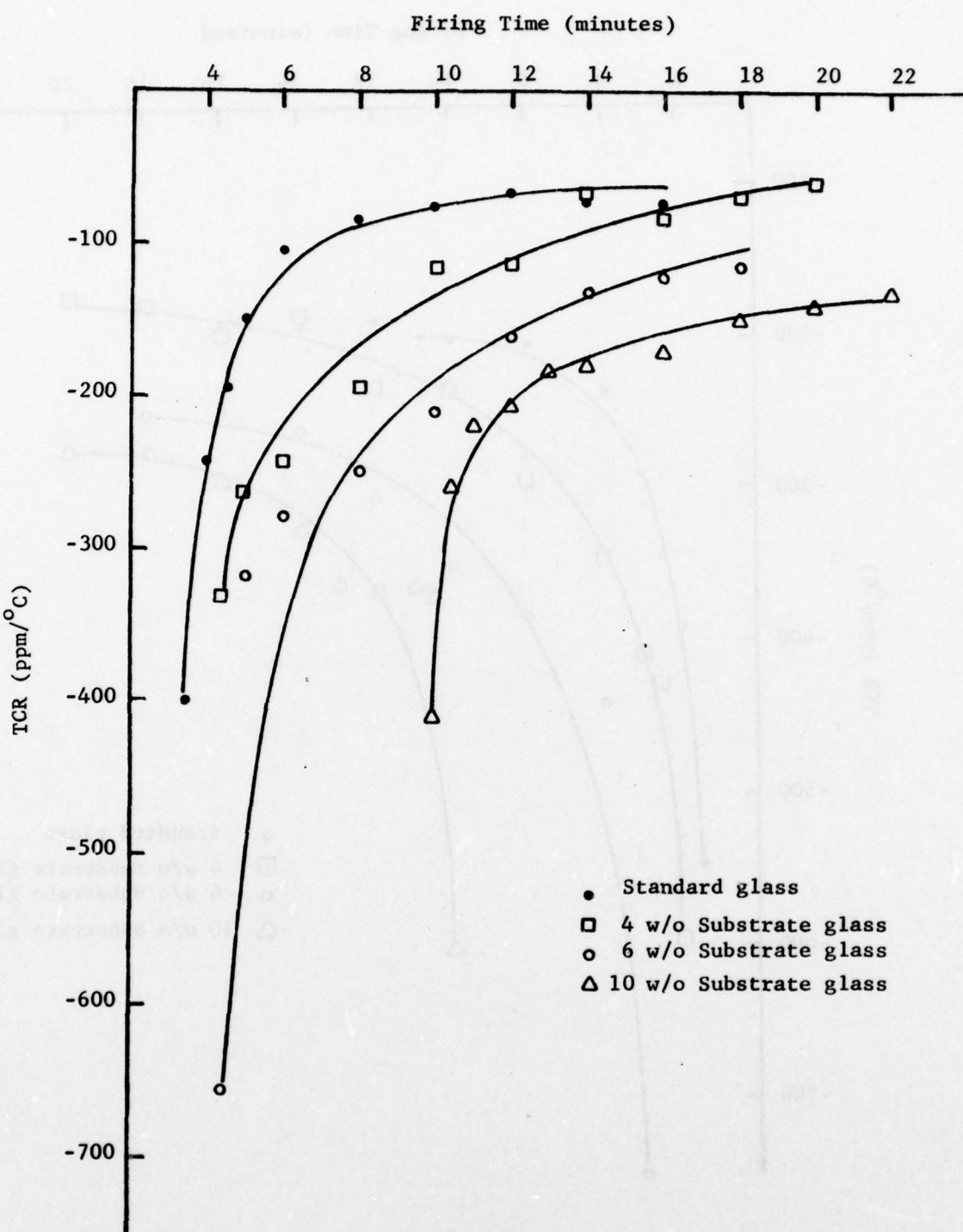


Figure 4. Hot ( $25^{\circ}$  to  $125^{\circ}\text{C}$ ) TCR versus Firing Time at  $800^{\circ}\text{C}$ .

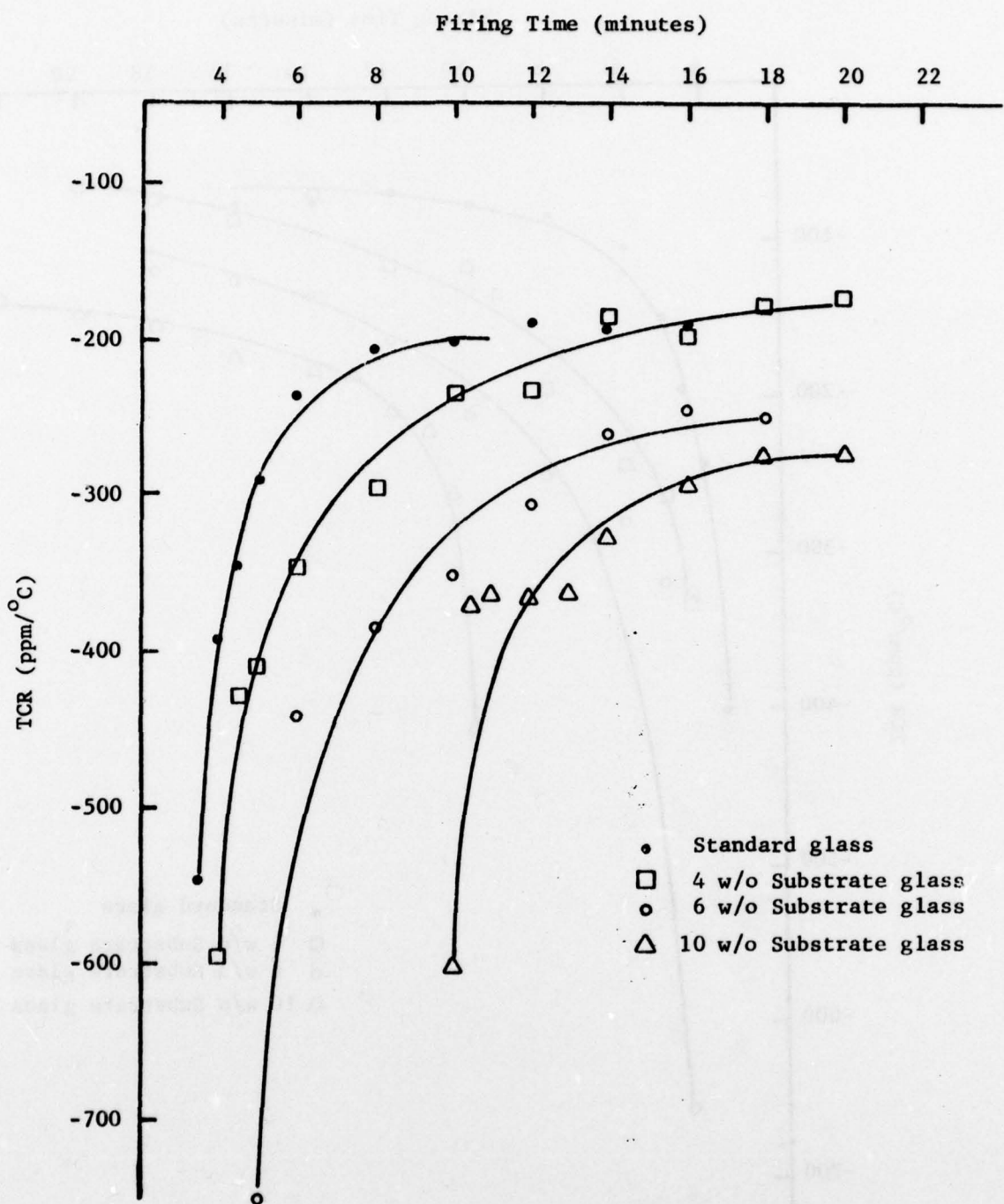


Figure 5. Cold (-55° to 25°C) TCR versus Firing Time at 800°C.

will have a large positive TCR whereas a non-sintered contact can have a TCR that is very large and negative. The second result is due to the reduced kinetics for microstructure development in resistors made from glasses with increasing substrate concentrations. The more substrate that is present the higher the viscosity of the glass which retards the network development and results in a higher number of non-sintered contacts relative to sintered contacts.

One resistor of each glass composition that had been fired at 800<sup>o</sup>C for 16 minutes was selected for determination of a more complete resistance versus temperature curve. These resistors were mounted on a copper block in order to establish thermal equilibrium and placed in an environmental chamber where the temperature was varied in 5 degree intervals from -55<sup>o</sup> to 125<sup>o</sup>C. The resistance was measured using a four terminal technique, and three heating and cooling cycles were conducted in order to establish the reproducibility of the experimental data. All resistance values were then normalized to their 25<sup>o</sup>C readings, and the results are plotted in Fig. 6 as a function of temperature. The curvature of the plots for each of the glass compositions increases with increasing amount of substrate dissolved in the glass and with decreasing temperature.

The four resistors used to obtain the data shown in Fig. 6 along with one other sample of each of the same compositions and firing times were immersed in liquid nitrogen and their resistances determined. The values for each composition were averaged and a TCR calculated. These results along with the sheet resistance and the hot and cold TCRs previously determined for these compositions are shown in Table 1.

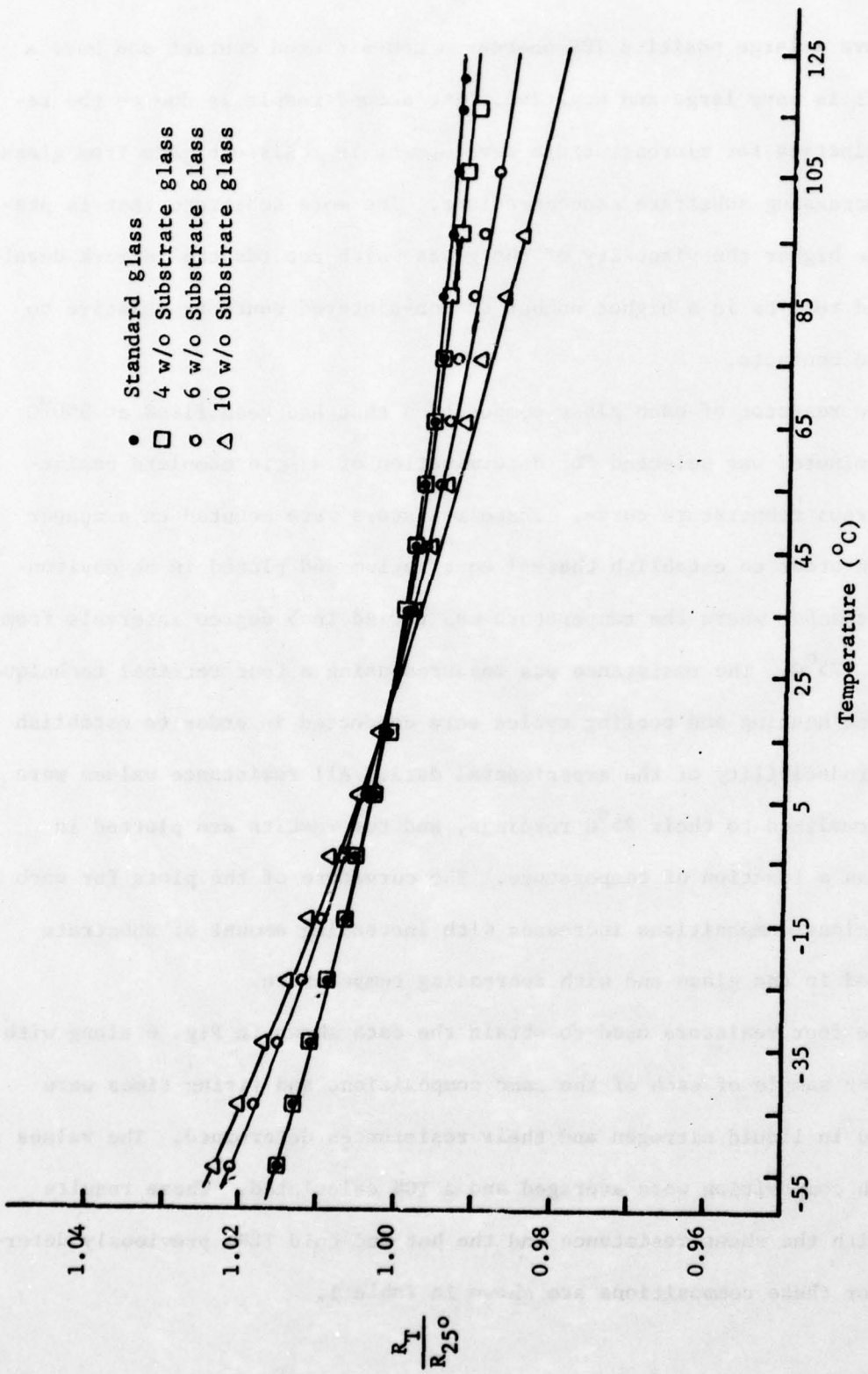


Figure 6. Temperature Dependence of Resistance for Resistors Fired at  $800^\circ\text{C}$  for 16 Minutes.

Table 1

TCR of 5 w/o RuO<sub>2</sub> Resistors Fired at 800°C for 16 Minutes

Resistor Glass	$R_s$ (KΩ/n-25μm)	TCR (ppm/°C)		
		-196° to 25°C	-55° to 25°C	25° to 125°C
Standard	146	-420	-190	- 75
4 w/o AlSiMag 614	604	-420	-195	- 80
6 w/o AlSiMag 614	717	-540	-250	-125
10 w/o AlSiMag 614	2300	-510	-285	-195

The observation of a more negative TCR with decreasing average temperature is consistent with a model of non-sintered thermally activated contacts as being integral parts of the resistor network.

#### 4.4 Current Noise

Any electrically conducting medium when viewed on a small enough scale will exhibit random fluctuations of voltage, current, and resistance called noise. Physically, these variations are caused by any mechanism that scatters charge carriers (lattice vibrations, grain boundaries, non-uniform internal electric fields, etc.). In thick film resistors, there are two major types of noise: thermal noise and current noise. Thermal noise is present in all materials and occurs whether or not there is an electric field applied. It is a function of temperature, bandwidth, and frequency. Current noise, however, is the more important of the two in thick film resistors, and is found to be the major contributor to the noise spectrum over the normal frequency range of use. Current noise is

inversely proportional to frequency so that for low frequency applications, i.e., in the audio range, the effect can be quite large. The resistors prepared by firing at constant temperature with varying time and those fired at constant time with varying temperature were tested for the noise characteristics. The Quantech noise test method (13) was employed to measure the noise index of each sample. The noise index (NI) in db in a decade of frequency is defined as follows:

$$NI = 20 \log (\sqrt{v^2}/V)$$

where  $\sqrt{v^2}$  is the rms current noise voltage measured in microvolts, and V is the DC applied voltage across the resistor measured in volts. From this equation, it can be seen that the 0db point corresponds to 1 microvolt of rms noise per volt of applied bias. The noise indices for resistors made with the standard glass and the standard plus 4, 6, and 10 weight percent dissolved substrate are shown in Fig. 7 for varying firing time at 800°C and in Fig. 8 for varying firing temperature for 10 minutes firing time.

The results shown in Figs. 7 and 8 are consistant with the microstructure development and charge transport model if it is assumed that the primary contributor to noise in thick film resistors is the non-sintered contacts in the resistor chains. If the noise is associated with the non-sintered contacts then an increase in firing time or temperature should lead to a decrease in the noise index because the number of non-sintered contacts relative to sintered contacts will decrease for either of these conditions. This decreasing noise index is observed in all eight curves on Figs. 7 and 8 during the initial stages of firing.

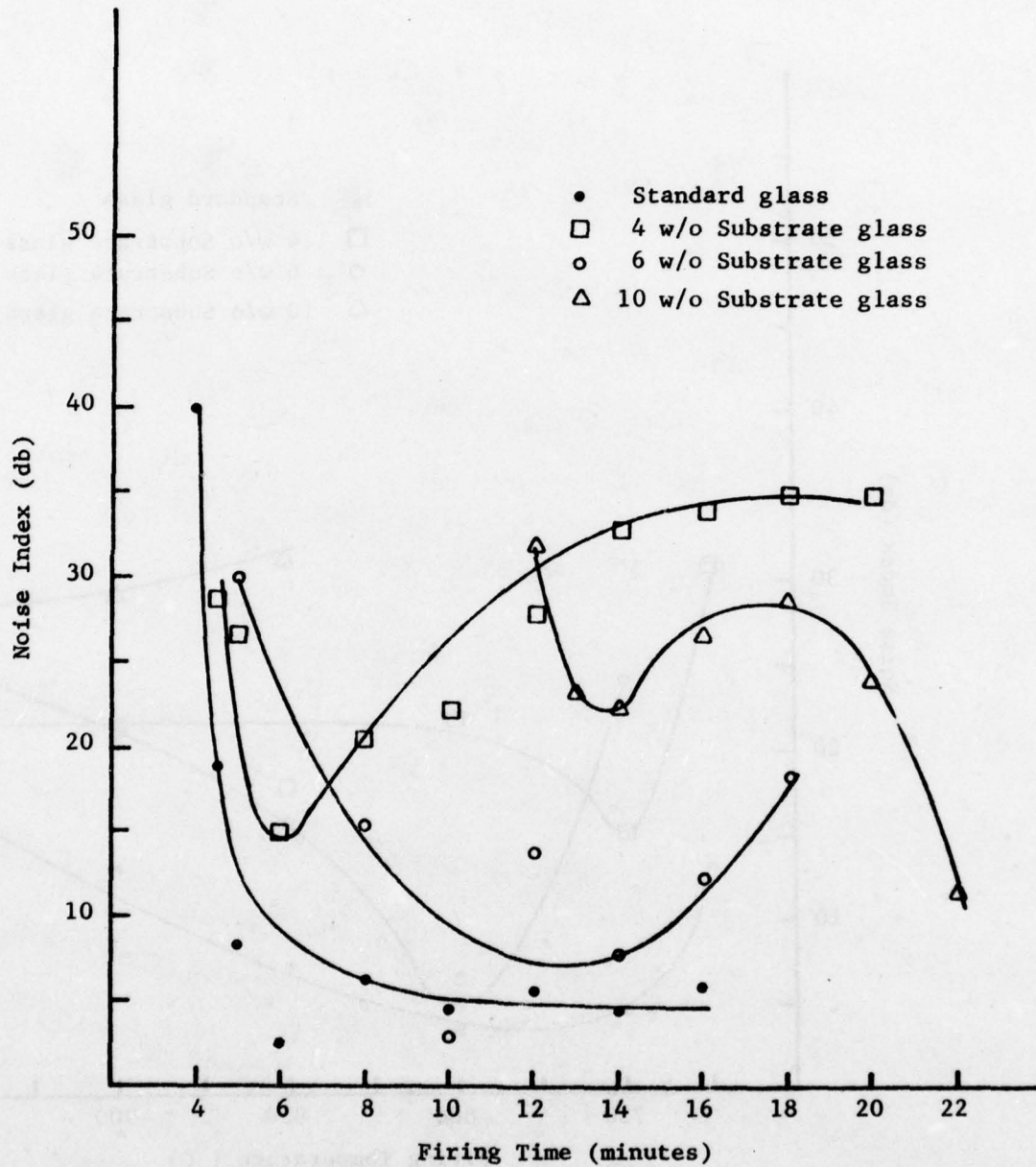


Figure 7. Current Noise versus Firing Time at 800°C.

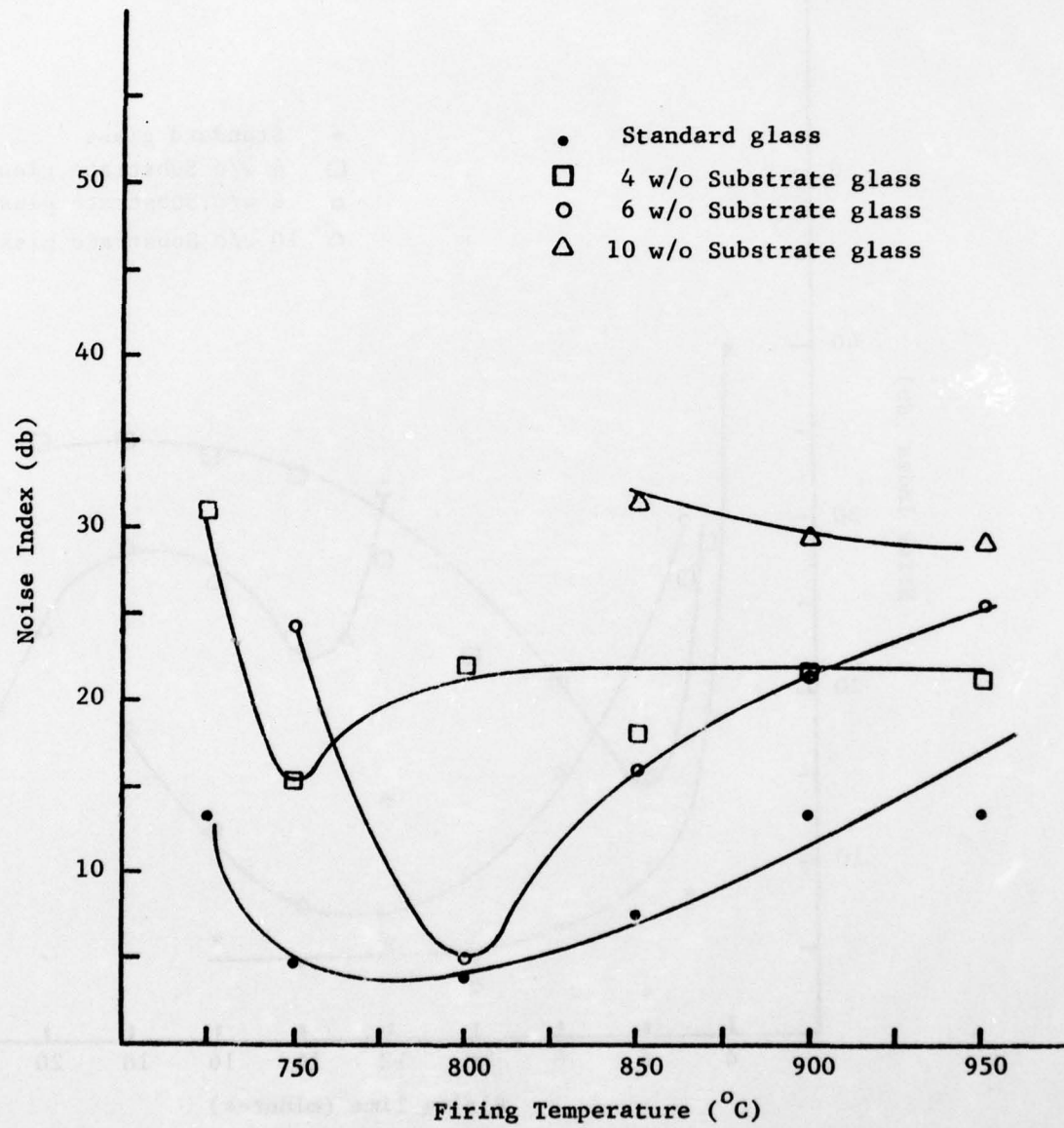
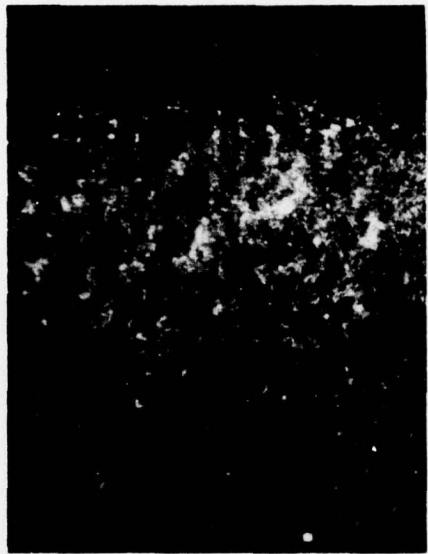


Figure 8. Current Noise versus Firing Temperature for 8 Minute Firing Time.

As the firing proceeds, the microstructure development model predicts a continued decrease in the noise index but at a slower rate. This type of behavior is shown by the standard glass resistors in Fig. 7 and the 10 w/o substrate glass resistors in Fig. 8, but all other curves on Figs. 7 and 8 show a minimum followed by an increase in the noise index. The 10 w/o substrate glass in Fig. 7 also shows a maximum followed by a second decrease in NI. This anomaly in the noise index can be associated with phenomena occurring at the resistor-conductor interface. Figures 9 through 12 are a series of photomicrographs of the interface between the conductor (top of the photomicrographs) and the resistor after different firing times at 800°C. The standard glass resistors, Fig. 9, show signs of a decreasing density of the opaque RuO<sub>2</sub> relative to the transparent glass in the resistor near the resistor-conductor interface at short times (Fig. 9a), but a more uniform distribution of RuO<sub>2</sub> pigment at longer firing times. The current noise for this resistor (Fig. 7) decreases rapidly at short times and remains constant for firing times greater than 8 minutes. A different behavior is seen with the 4 w/o substrate glass resistors, shown in Fig. 10. A relatively uniform conductor-resistor interface is observed at shorter firing times, e.g., 4 and 6 minutes, but a longer firing times a thinning of the RuO<sub>2</sub> pigment in the resistor near the resistor-conductor interface is observed. This thinning reaches very severe proportions after 14 minutes at 800° (Fig. 10d); a firing condition which also corresponds to a maximum in the current noise (see Fig. 7). The 6 and 10 w/o substrate glass resistors also show changes in the RuO<sub>2</sub> density near the resistor-conductor interface, as can be seen in Figs. 11



a. 3.5 minutes



b. 8 minutes

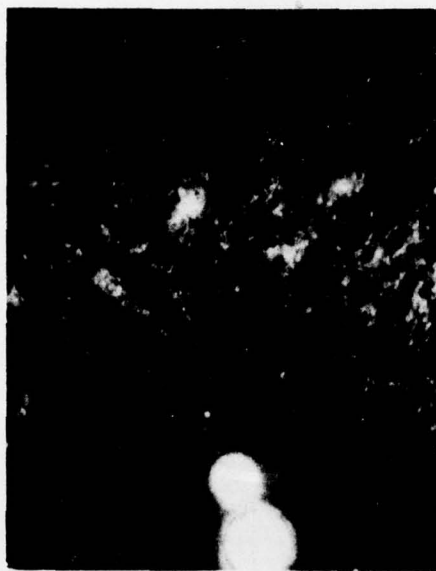


c. 12 minutes

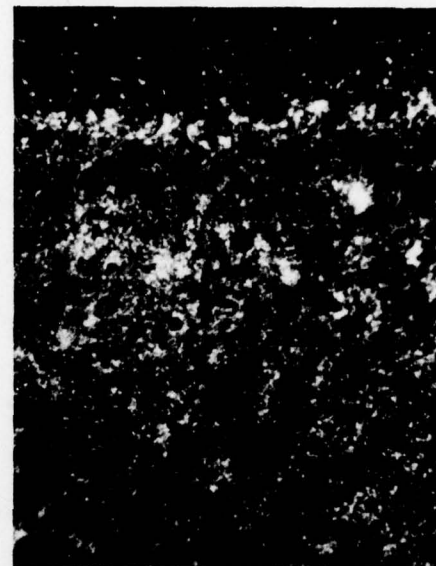


d. 16 minutes

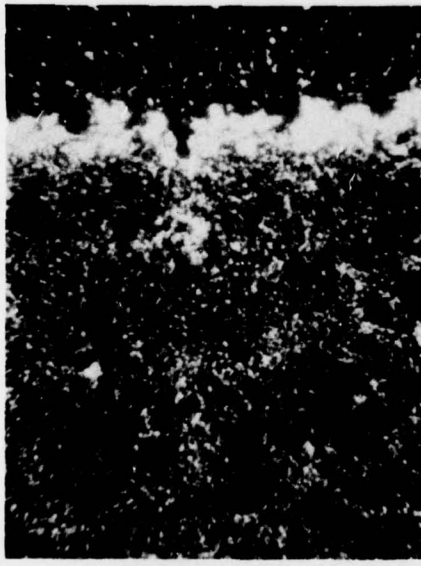
Figure 9. Resistor-Conductor Interface in Standard Glass Resistors Fired for Varying Time at 800°C.



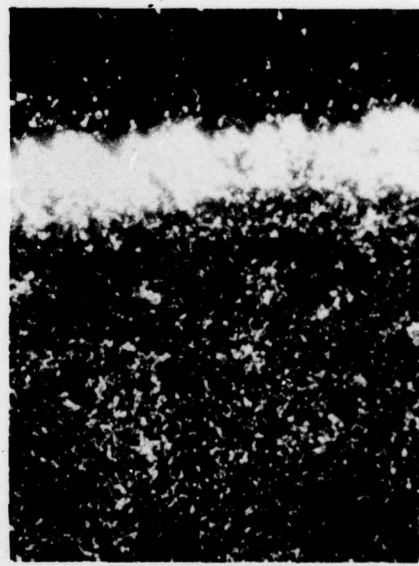
a. 4 minutes



b. 6 minutes

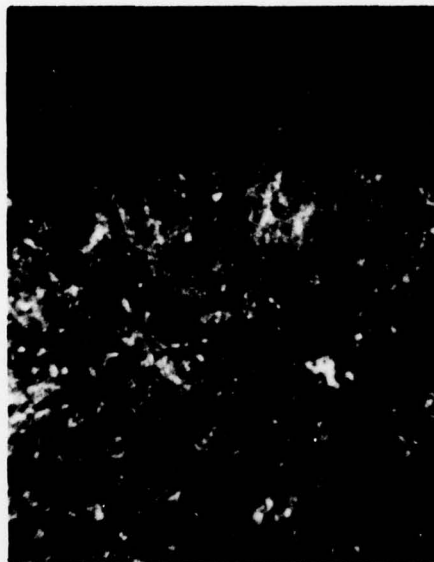


c. 10 minutes

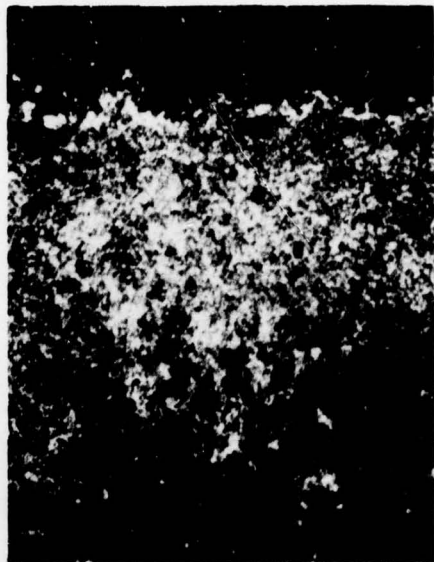


d. 14 minutes

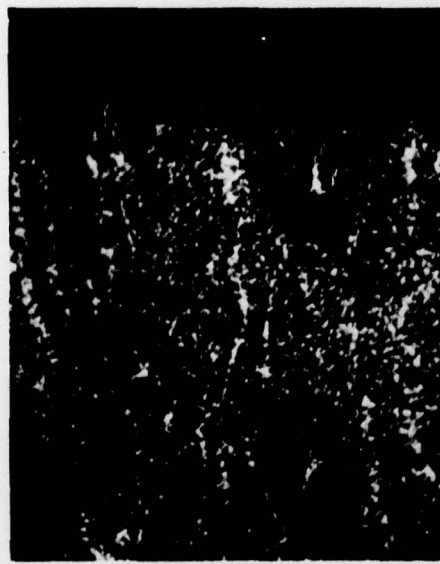
Figure 10. Resistor-Conductor Interface in 4 w/o Substrate Glass  
Resistors Fired for Varying Time at 800°C.



a. 4 minutes



b. 6 minutes

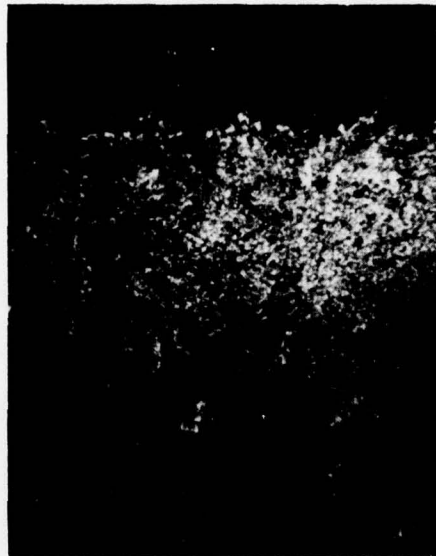


c. 14 minutes



d. 18 minutes

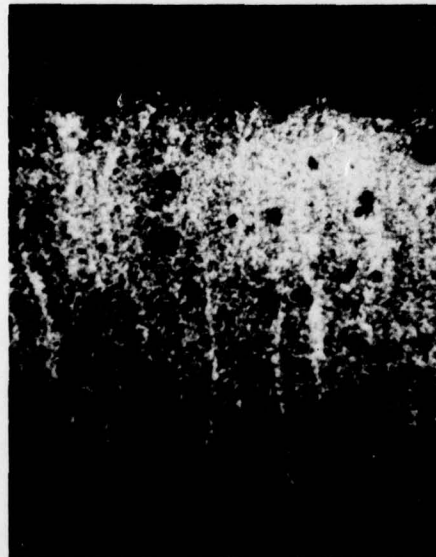
Figure 11. Resistor-Conductor Interface in 6 w/o Substrate Glass  
Resistors Fired for Varying Time at 800°C.



a. 10 minutes



b. 14 minutes



c. 18 minutes



d. 22 minutes

Figure 12. Resistor-Conductor Interface in 10 w/o Substrate Glass  
Resistors Fired for Varying Time at 800°C.

and 12. The 10 w/o substrate glass resistors show a maximum in pigment thinning near 18 minutes firing time with a more uniform RuO<sub>2</sub> density at both shorter and longer times, which correlates with the maximum in the noise index for this composition shown in Fig. 7.

## 5. MIM STUDIES

### 5.1 Experimental

Metal-insulator-metal (MIM) devices are being fabricated after several modifications in the originally proposed (2) experimental procedure. Sputtered platinum electrodes were found to be unsuitable due to fringing around the metal mask, which led to unacceptable pattern definitions. The electrode material was changed to evaporated gold in order to circumvent this problem. The substrate used with the modified procedure is an oxidized silicon wafer coated with a layer of chromium prior to gold deposition in order to insure adequate adhesion. The glass is RF sputtered in a argon-oxygen atmosphere, and the top gold electrodes are evaporated in a dot pattern after the glass film has been annealed in oxygen.

The anneal step is necessary because it is possible that some of the PbO in the glass could be disassociated into elemental lead during the sputtering operation. In addition, stresses could develop in the film due to the high energy impact between sputtered glass molecules and the existing film, and the density of the film may be lower than that of bulk glass because of the sputtering deposition. Experiments to determine a proper temperature and time for annealing the sputtered films are being carried out in an oxygen atmosphere, and temperatures are selected with reference to the results of studies of viscosity as a function of composition (4). The annealing point, defined as the temperature at which the viscosity is  $10^{12}$  Pa·s, is  $446^{\circ}\text{C}$  for the standard glass; internal strains should be relieved in approximately 15 minutes at this temperature. The devices are annealed by placing the wafers in a fused quartz boat in a

pyrex lined, resistively heated furnace at 380°C or 440°C with a constant flow of oxygen. The anneal times investigated to date were 30 minutes, 1, 2, 4, 6, and 8 hours accumulative, that is, a one hour anneal is the initial 30 minute anneal plus a second 30 minute anneal after electrical testing.

In order to compare the dielectric constant and conductivity of the sputtered film and bulk glass, parallel plate capacitors were made with the standard glass. A quantity of 63-25-12 glass was melted in a platinum crucible at 900°C and poured into a heated stainless steel mold. The mold was allowed to cool to room temperature, and the casting examined for cracks, bubbles, or devitrification. Good quality glass blanks were then annealed at 450°C for 16 hours in air. A cylinder, 7.5 mm diameter, was cut from the blank using a diamond core drill, and the cylinder was sliced into 0.3 to 0.8 mm thick sections using a slow speed diamond saw. The samples were then polished and provided with evaporated gold electrodes.

The complex admittance and dissipation factor are being measured as a function of frequency using a General Radio, GR 1615-A capacitance bridge. The samples to be studied are placed on a vacuum chuck in a light tight, grounded metal box. A micro-positioner with a tungsten probe is used to make contact to the lower electrode at a corner of the sample where the glass has been etched away. A second micro-positioner with a 76  $\mu$ m gold wire is used to make contact to the top electrodes of the devices. All leads emerging from the metal box are coaxial cable. The GR 1615-A bridge measures either series capacitance ( $C_s$ ) and dissipation factor ( $D$ ) or the parallel capacitance ( $C_p$ ) and parallel conductance ( $G_p$ ). However, these quantities and the admittance ( $Y$ ) are all interrelated through the following formulas.

$$Y = G_p + jwC_p$$

$$D = G_p / wC_p$$

$$C_s = (w^2 C_p^2 + G_p^2) / w^2 C_p$$

$$C_p = C_s / (1 + D^2)$$

$$G_p = wC_s D / (1 + D^2)$$

## 5.2 Results and Discussion

Figures 13-16 summarize the preliminary results from the anneal experiments. Figure 13 shows that the parallel capacitance and conductance both decrease as the annealing time increases at 380°, but that little change occurs in either quantity after two hours of anneal. Figure 14 shows the parallel capacitance and conductance as a function of frequency for a virgin and an annealed MIM, and for a bulk glass sample which was also annealed at 440°C for 30 minutes. There is again a decrease in capacitance and conductance with annealing of the MIM device, and a decrease in the frequency dependence of  $C_p$  approaching the frequency independent behavior exhibited by the bulk glass sample. The dissipation factors corresponding to the data of Figs. 13 and 14 are plotted in Figs. 15 and 16 respectively. There is a suggestion of a minimum in the dissipation factor curves at approximately 10 kHz which may be indicative of a transition from a dissipation factor dominated by DC conductance, which would produce an inverse frequency dependence, to a dielectric loss mechanism which would produce a maximum at some higher frequency. The measurements must be extended to both lower and higher frequencies in order to investigate this type of behavior.

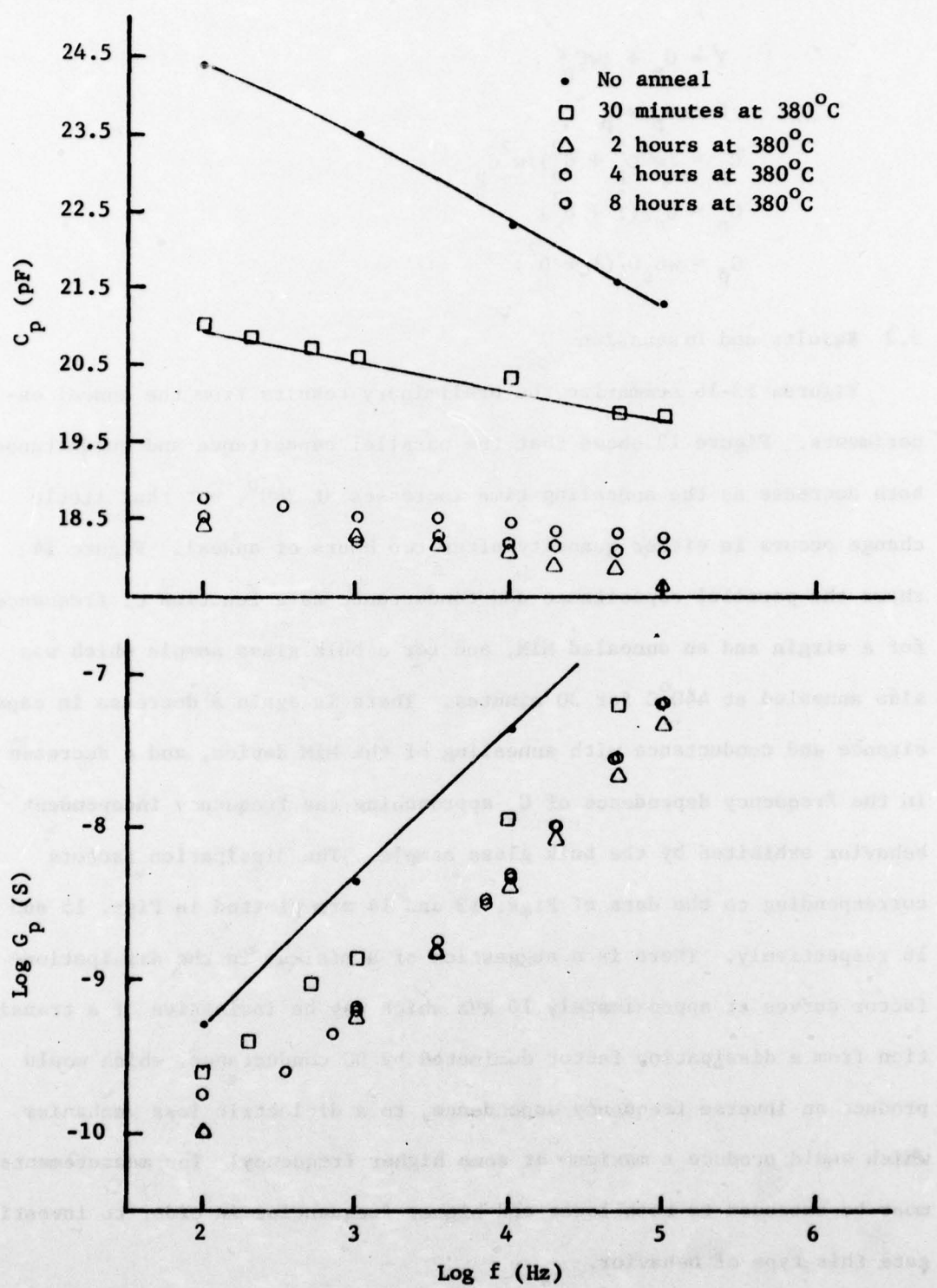


**Figure 13. Parallel Conductance and Capacitance of MIM Devices with Standard Glass.**

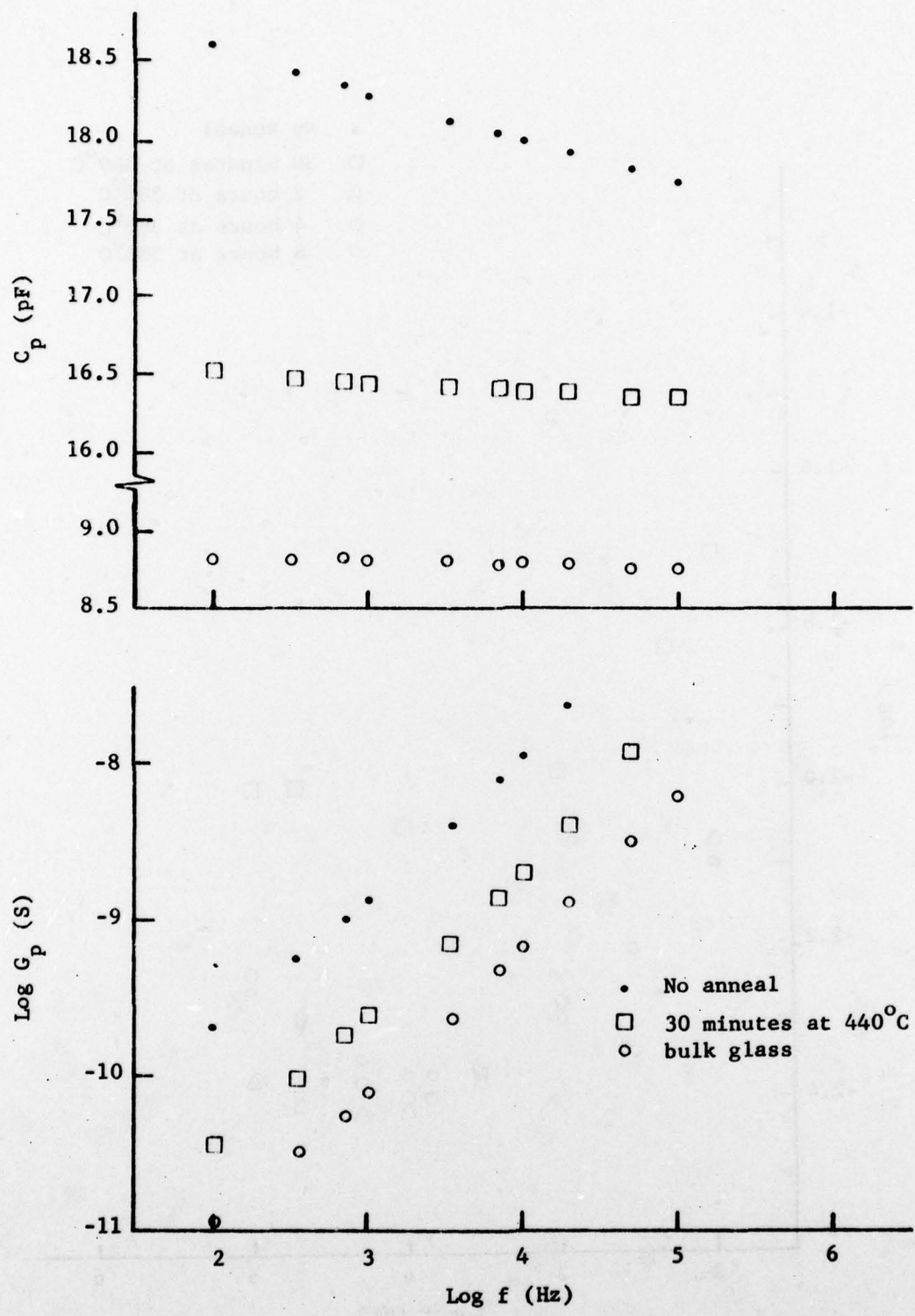


Figure 14. Parallel Conductance and Capacitance of MIM Devices and Bulk Standard Glass.

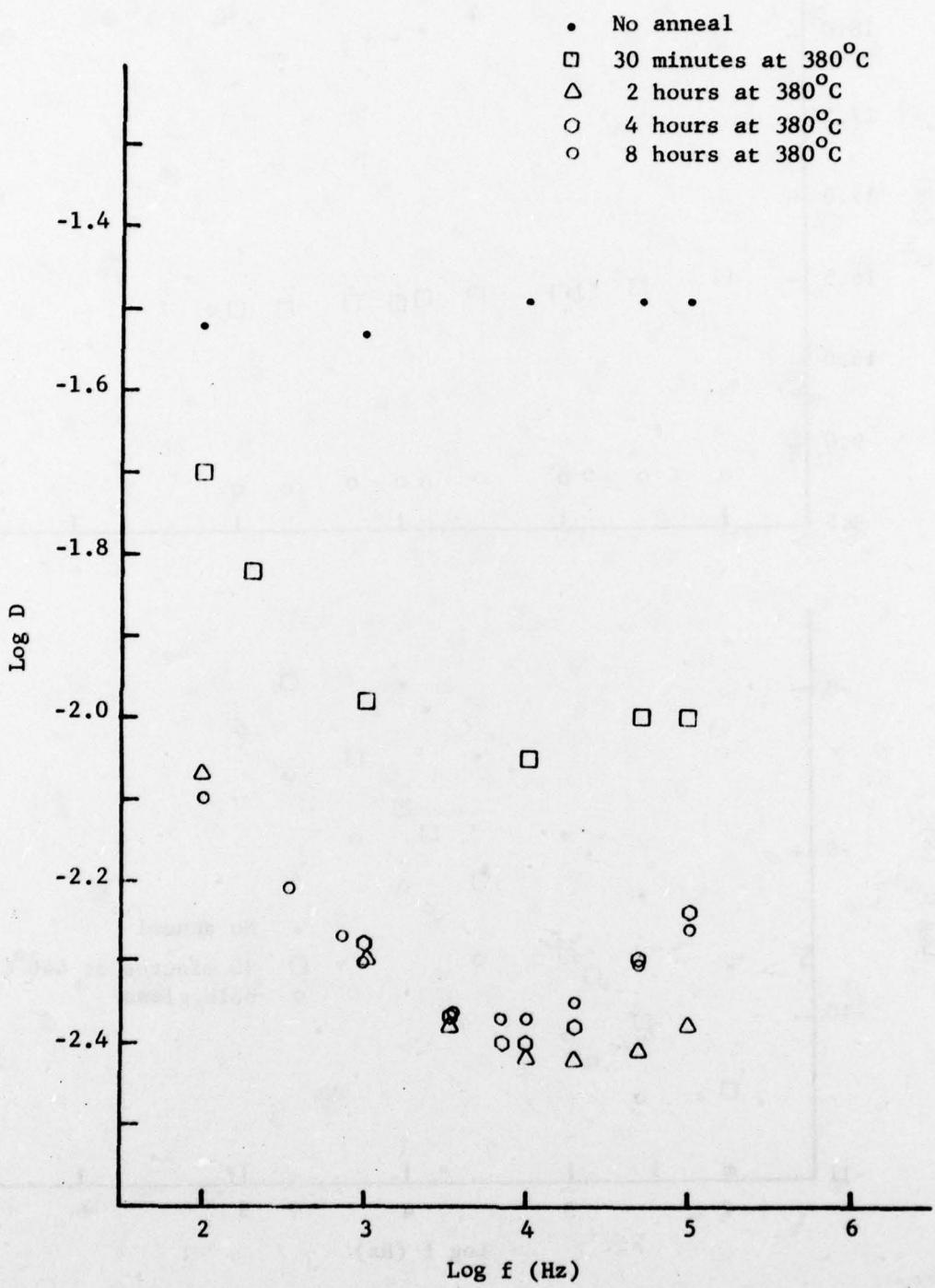


Figure 15. Dissipation Factor for Standard Glass MIM Devices Annealed at  $380^{\circ}\text{C}$ .

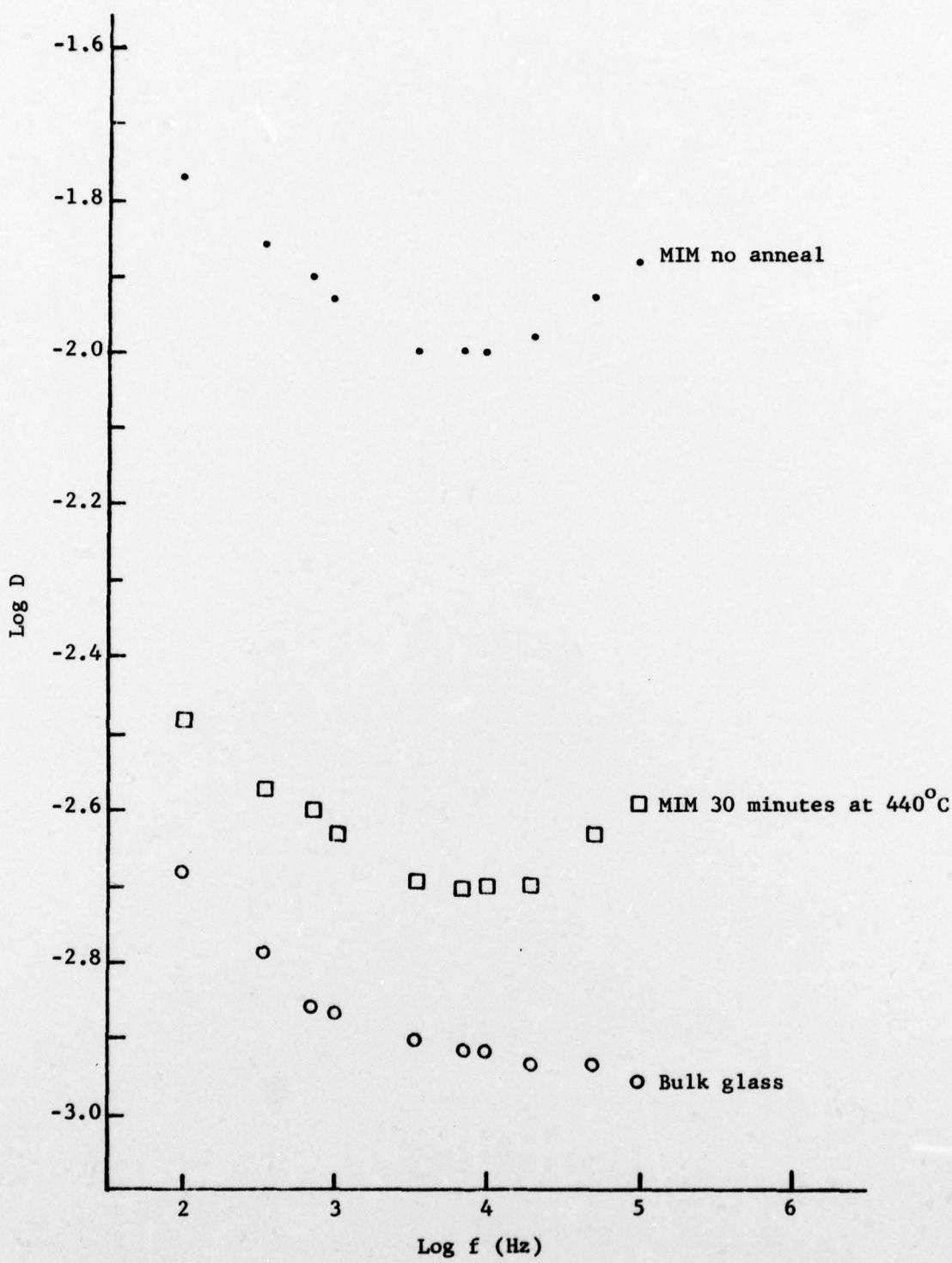


Figure 16. Dissipation Factor for Standard Glass MIM Devices and in Bulk.

## 6. REFERENCES

1. R. W. Vest, "The Effects of Substrate Composition on Thick Film Circuit Reliability," Final Technical Report on Contract No. N00019-76-C-0354, 28 February 1977.
2. R. W. Vest, "The Effects of Substrate Composition on Thick Film Circuit Reliability," Final Technical Report on Contract No. N00019-77-C-0327, 28 February 1978.
3. R. W. Vest, "The Effects of Substrate Composition on Thick Film Circuit Reliability," Quarterly Report No. 1 on Contract No. N00019-78-C-0236, 30 May 1978.
4. R. W. Vest, "The Effects of Substrate Composition on Thick Film Circuit Reliability," Quarterly Report No. 2 on Contract No. N00019-78-C-0236, 31 August 1978.
5. A. N. Prabhu and R. W. Vest, "Investigation of Microstructure Development in RuO<sub>2</sub>-Lead Borosilicate Glass Thick Films," *Mat. Sci. Res.*, 10, 399-408 (1975).
6. R. W. Vest, "Conduction Mechanisms in Thick Film Microcircuits," Final Technical Report, Purdue Research Foundation Grant Nos. DAHC-15-70-G7 and DAHC-15-73-G8, ARPA Order No. 1641, December 1975, pp. 168-187.
7. Reference 6, pp. 149-52.
8. J. Mukerji and S. R. Biswas, "Solubility of Ruthenium in Soda Silicate Glasses," *Cent. Glass Cer. Res. Ins. Bull.*, 14, 30 (1967).
9. K. K. Dhasgupta and J. Mukerji, "Solubility Dependence of Ruthenium Volatilization from Glass," *Trans. Ind. Cer. Soc.*, 27, 123 (1968).
10. A. Prabhu, G. L. Fuller and R. W. Vest, "Solubility of RuO<sub>2</sub> in a Pb Borosilicate Glass," *J. Am. Ceram. Soc.*, 57 (9), 408-9 (1974).
11. Reference 6, p. 253.
12. Reference 6, pp. 244-306.
13. G. T. Conrad, Jr., N. Newman and A. P. Stansbury, "A Recommended Standard Resistor-Noise Test System," *IRE Transactions on Component Parts*, CP-7 (3), 1-18 (1960).

## 7. FUTURE PLANS

Viscosity and surface tension as a function of glass composition and temperature will be measured at higher temperatures. The kinetics of ripening of RuO<sub>2</sub> in the glass will be determined as a function of glass composition and the kinetics of the initial stage of liquid phase sintering of RuO<sub>2</sub> will be calculated from the ripening data and the solubility data. These results will then be correlated utilizing the previously developed models for microstructure development, and the influence of glass composition established. The effects of substrate dissolution on charge transport processes in non-sintered contacts will be determined by fabricating metal-insulator-metal (MIM) structures with different glass compositions and measuring the dielectric properties, bulk resistivity and breakdown characteristics of the glass as well as the current-voltage characteristics of the MIM. The dependence of both the glass properties and the electrical properties of the non-sintered contacts on glass composition will be incorporated into a revised charge transport model for thick film resistors.

## 8. STATEMENT OF ESTIMATED COSTS

Contract No. N00019-78-C-0236

February 1, 1978 - January 31, 1979

Beginning Fund Balance	\$ 65,000.00
Funds Expended Through 10/31/78	<u>33,298.83</u>
Funds Remaining	\$ 31,701.17

### Planned Expenditures (Approximate)

November	\$15,900
December	7,900
January	7,900